

## Protective effect of the *Rubus chingii* Hu. fruit extract on ultraviolet B-induced photoaging via suppression of mitogen-activated protein kinases (MAPKs) *in vitro*

Jie-Mei She<sup>1</sup>, Hui-Hui Yuan<sup>1,2,\*</sup>, Jin Zhang<sup>3</sup>, Zhao-Nian Si<sup>1</sup> and Min-Bo Lan<sup>1,4,#</sup>

<sup>1</sup>Shanghai Key Laboratory of Functional Materials Chemistry, School of Chemistry & Molecular Engineering, East China University of Science and Technology, Shanghai 200237, China

<sup>2</sup>Institute of Applied Chemistry, East China University of Science and Technology, Shanghai 200237, China

<sup>3</sup>Shanghai Putuo Hospital of Traditional Chinese Medicine, Shanghai 200062, China

<sup>4</sup>State Key Laboratory of Bioreactor Engineering, East China University of Science and Technology, Shanghai 200237, China

**Corresponding authors:** \*yuanhuihui@ecust.edu.cn; #minbolan@ecust.edu.cn

**Received:** March 21, 2019; **Revised:** May 3, 2019; **Accepted:** June 3, 2019; **Published online:** July 7, 2019

**Abstract:** *Rubus chingii* Hu. is an important traditional Chinese medicine with a beneficial effect on the kidney. Traditional Chinese medicine theory believes that supporting the kidney has a key role in anti-aging. To the best of our knowledge, the anti-photoaging activity of *Rubus chingii* Hu. has not been investigated. We investigated the anti-photoaging effects and the underlying mechanism of the ethyl acetate fraction of *Rubus chingii* Hu. fruit ethanol extract (E-EA) in UVB-induced human fibroblasts (HFF-1). Our results show that E-EA (10-40 µg/mL) displayed preventive and therapeutic effects on UVB-induced cytotoxicity in HFF-1 cells. E-EA also presented significant anti-photoaging properties in UVB-induced HFF-1 cells by decreasing the levels of reactive oxygen species (ROS), inhibiting matrix metalloproteinase 1 (MMP-1) production and promoting type-I procollagen production via suppression of the mitogen-activated protein kinase (MAPK) signaling pathway. These results suggested that E-EA might be a promising anti-photoaging agent to protect the skin from UVB damage, with a potential application in cosmetics.

**Keywords:** *Rubus chingii* Hu.; antioxidant activity; anti-photoaging; reactive oxygen species (ROS); mitogen-activated protein kinase (MAPK) signaling pathway

## INTRODUCTION

Skin, the largest organ of body, acts as a physical and immunological barrier against harmful environmental factors such as ultraviolet (UV) radiation, pathogens and toxicants [1]. UV radiation is classified into UVA (320-400 nm), UVB (280-320 nm) and UVC (200-280 nm). UVB is the commonest and most harmful external component that threatens the skin and results in skin photoaging [2, 3]. Prolonged exposure to UVB has been reported to cause acute and chronic skin damage such as dryness, reddening, sunburn, roughness, thickening, wrinkling, and skin cancer [4]. Natural plant extracts are widely used as cosmetic ingredients because of their capability to slow skin decline [5], and the search for natural principles is attracting an ever-growing interest in skin care.

UVB stimulation of the skin leads to oxidative stress, which in turn causes overproduction of reactive oxygen species (ROS) and damages the endogenous antioxidant defense system [1,2]. The overproduction of ROS causes lipid peroxidation, DNA damage, and critical structural and functional protein changes, all of which result in cell damage [1,2]. Moreover, the overproduction of ROS activates the mitogen-activated protein kinases (MAPK) signaling pathway, including the extracellular signal-regulated kinases (ERK), c-Jun N-terminal kinases (JNK) and p38, and increases the expression of matrix metalloproteins (MMPs), thereby promoting collagen degradation. [6,7]. Collagen produced by fibroblasts is the main structural protein in the dermal extracellular matrix (ECM), which is responsible for adherence to connective tissues and the tensile strength of skin [7]. Loss of collagen will

cause wrinkles on the skin [7]. Oxidative stress plays an important role in UVB-induced skin photoaging. Therefore, exogenous supplementation of antioxidants to decrease ROS overproduction was considered as an effective strategy against photoaging [1].

*Rubus chingii* Hu., a member of the Rosaceae family, is a traditional medicinal plant used in China to treat renal asthenia, frequent urination, premature ejaculation and erectile dysfunction [8]. Aging is associated with a decline in health and integrity of the human kidney [9]. According to traditional Chinese medicine theory, reinforcing kidney functions has a key role in anti-aging. A glycoprotein purified from *Rubus chingii* Hu. provides potential anti-aging activities by improving klotho gene expression and improving kidney function [8]. *Rubus chingii* Hu. could protect against photoaging according to its beneficial medicinal effect on the kidneys. In addition, the anti-aging properties of plants are attributed to their antioxidants, which minimize ROS overproduction and protect skin against solar radiation [5]. Improved ROS equilibrium can reduce the risk of kidney damage [10] and cell aging [11]. *Rubus chingii* Hu. has been reported to contain flavonoids with significant antioxidant and protective effects against disease induced by oxidative stress [12-14]. Furthermore, *Rubus chingii* Hu. shows antiinflammatory activity through the suppression of MAPK activation in macrophages [15]. However, to the best of our knowledge, the anti-photoaging activity of *Rubus chingii* Hu. has not been investigated so far.

In this study, the anti-photoaging properties of *Rubus chingii* Hu. fruit extract were investigated. The optimum solvent fraction was identified by measuring the antioxidant activity of various *Rubus chingii* Hu. fruit fractions. The preventive and therapeutic effects of the fraction on UVB-induced cytotoxicity in human fibroblasts (HFF-1) were evaluated by the (3-(4,5-dimethylthiazol-2-yl)-2,5-diphenyltetrazolium) (MTT) method. Furthermore, its effect on ROS, MMP-1 and type-I procollagen expression were investigated and the underlying molecular mechanisms on the MAPK signaling pathway were evaluated in UVB-induced HFF-1 cells. Finally, the main flavonoid components of the optimum solvent fraction were determined by HPLC.

## MATERIALS AND METHODS

### Chemicals and reagents

Dried fruit of *Rubus chingii* Hu. was purchased from Leiyunshang Pharmaceutical Co. Ltd (Shanghai, China). Rutin, hyperin, quercetin and kaempferol were purchased from Aladdin Industrial Corporation (Shanghai, China). Dulbecco's modified Eagle's medium (DMEM), fetal bovine serum (FBS), 0.25% (w/v) trypsin and penicillin streptomycin were obtained from Gibco-BRL (Gaithersburg, MD, USA). Enzyme-linked immunosorbent assay (ELISA) kits for MMP-1 and type-I procollagen were purchased from Shanghai Meilian Biotechnology Co. Ltd., China. Antibodies against p-ERK, p-JNK, p-p38, ERK, p38 and  $\beta$ -actin were obtained from Cell Signaling Technology (Danvers, MA, USA). Antibodies against JNK were obtained from Proteintech (Chicago, IL, USA).

### Preparation of *Rubus chingii* Hu. extract

Air-dried fruits of *Rubus chingii* Hu. were collected from Zhejiang, China. Twenty g of the dried fruit were macerated in 200 mL ethanol (80%) for 30 min at room temperature and extracted with 80% ethanol (3 $\times$ 200 mL) for 2 h under reflux conditions. The filtrates were combined, concentrated and lyophilized to obtain the *Rubus chingii* Hu. ethanol extract (E; 3.52 g). Three g of E were suspended in methanol/deionized water (v/v, 1:1, 150 mL) and extracted successively with 150 mL petroleum ether, ethyl acetate and n-butyl alcohol 3 times. The organic phases and water phase were concentrated and lyophilized to obtain the petroleum ether fraction (E-PE; 0.29 g), the ethyl acetate fraction (E-EA; 0.93 g), the n-butanol fraction (E-NB; 0.58 g), and the residual water fraction (E-WR, 0.81 g).

### DPPH radical scavenging assay

DPPH radical scavenging capacity was evaluated as described [16]. Two mL of the extract (1.25, 2.5, 5, 10, 20, 40, 80, 100  $\mu$ g/mL) were added to 2.0 mL ethanol solution of the DPPH radical (0.1 mmol/L). The mixture was shaken and left to stand at room temperature and in the dark. After 30 min, the absorbance of the mixture was measured at 517 nm using a UV-vis spectrophotometer (CARY 300, Agilent

Technologies, USA) against an ethanol blank. Trolox (6-hydroxy-2,5,7,8-tetramethylchroman-2-carboxylic acid), a water-soluble analog of vitamin E, was used as positive control. DPPH radical scavenging capacity was calculated by the following formula:

$$I (\%) = \frac{A_b - A_s}{A_b} \times 100$$

where  $A_b$  is the absorbance of control, and  $A_s$  is the absorbance of sample/positive control. All assays were tested in triplicate, and the results were expressed as  $IC_{50}$  (samples at the concentration decrease the absorbance by 50%). The lower the  $IC_{50}$  value, the better the free radical scavenging activity.

### ABTS<sup>+</sup> radical scavenging assay

ABTS<sup>+</sup> radical scavenging capacity of samples was determined according to the literature with a little modification [17]. The ABTS<sup>+</sup> solution was obtained by mixing equal parts ABTS (7.0 mmol/L, aqueous solution) and  $K_2S_2O_8$  (2.45 mmol/L, aqueous solution) for 12 h reaction in dark conditions. Before the test, the ABTS<sup>+</sup> solution was diluted with deionized water to obtain a diluted ABTS<sup>+</sup> solution with an absorbance of about  $0.7 \pm 0.05$  (734 nm). One mL of the sample with different concentrations (1.25, 2.5, 5, 10, 20, 40, 80, 100  $\mu\text{g/mL}$ ) was mixed with 1.0 mL diluted ABTS<sup>+</sup> solution for 10 min in the dark. The absorbance (734 nm) of the mixture was measured using the UV-vis spectrophotometer. Trolox was used as the positive control. ABTS<sup>+</sup> radical scavenging capacity was calculated by the following formula:

$$I (\%) = \frac{A_b - A_s}{A_b} \times 100$$

where  $A_b$  is the absorbance of control, and  $A_s$  is the absorbance of the sample/positive control. All assays were tested in triplicate, and the results were expressed as  $IC_{50}$ .

### The total reducing power assay

The total reducing power was measured by ferric reducing antioxidant power (FRAP) according to the literature with a little modification [18]. 2.5 mL of phosphate buffer (0.2 mol/L, pH 6.6) and 2.5 mL  $K_3Fe(CN)_6$  (1%, w/v) were added to 2.5 mL of sample solution (50  $\mu\text{g/}$

mL). The mixture solution was shaken and incubated at 50°C water bath for 20 min, and then cooled by ice water. 2.5 mL trichloroacetic acid (10%, w/v), 2.5 mL deionized water and 0.5 mL  $FeCl_3$  solution (0.1%, w/v) were added to the mixture solution for 10 min. The absorbance (700 nm) was measured against the solvent blank. The total reducing power was calculated using a Trolox standard for the calibration curve of five points from 6.25 to 100  $\mu\text{g/mL}$  ( $y = 0.00739x + 0.024$ ,  $R = 0.99929$ ). The total reducing power was expressed as Trolox equivalents in g/g of extract. All assays were run in triplicate.

### The total flavonoid content assay

The total flavonoid content (TFC) was measured colorimetrically [19]. Briefly, 100  $\mu\text{L}$  sample (10 mg/mL) were mixed with 4 mL deionized water, 0.3 mL  $NaNO_2$  solution (5%, w/v) and 0.3 mL  $AlCl_3$  solution (10%, w/v). The mixture was mixed and allowed to stand at room temperature for 6 min. To this, 2 mL  $NaOH$  solution (1 mol/L) was added and diluted with deionized water to a final volume of 10 mL. The absorbance (510 nm) of the mixture was measured 10 min later against the solvent blank. Quantifications were calculated using a rutin standard for the calibration curve of five points from 10.0 to 80.0  $\mu\text{g/mL}$  ( $y = 0.01274x - 0.03297$ ,  $R = 0.99978$ ). The total flavonoid content was expressed as rutin equivalents in mg/g of extract.

### UV absorption

The UVB absorption spectra of E-EA and Trolox were determined according to the method described previously [4]. Briefly, the UV absorption spectrum for the samples (200  $\mu\text{g/mL}$  in ethanol) was measured using a UV-vis spectrophotometer over a wavelength range of 200-400 nm. The blank (ethanol) was subtracted from the background reading.

### Cell culture

HFF-1 cells were kindly provided by Stem Cell Bank, Chinese Academy of Sciences (Shanghai, China). The HFF-1 cells were cultured in DMEM with 15% FBS and 100 U/mL penicillin-streptomycin at 37°C, 5%  $CO_2$  in a humidified incubator.

## UVB irradiation

The HFF-1 cells were washed with 250  $\mu$ L PBS twice and covered with 50  $\mu$ L PBS. Immediately, the HFF-1 cells were irradiated with different doses of UVB (312 nm). The UVB doses were determined with an UV-340 meter (Lutron, Taiwan, China). After irradiation, PBS was removed, and the cells were cultured in FBS-free medium for 24 h. Cells without UVB treatment were used as blank controls.

## Drug treatments

HFF-1 cells ( $5 \times 10^3$  cells/well) were seeded in 96-well plates and incubated overnight. Subsequently, HFF-1 cells were treated with E-EA (1.25-400  $\mu$ g/mL or 10-40  $\mu$ g/mL) in FBS-free medium for 24 h. Cells treated with UVB without drug treatment served as negative controls.

## Cell viability assay

The cell viability of HFF-1 was determined using the MTT assay. After incubation, the cells with or without any treatment were incubated with 200  $\mu$ L 0.5 mg/mL MTT in FBS-free medium for 4 h. The medium was removed and 150  $\mu$ L DMSO was added into each well to dissolve the formazan crystals. After shaking for 1 min, the plate was read at 492 nm using a multimode microplate reader (SpectraMax M2, Molecular Devices, Silicon Valley, CA). Cell viability was calculated by the following formula:

$$I (\%) = \frac{A_s}{A_b} \times 100$$

where  $A_b$  is the absorbance of the solvent control and  $A_s$  is the absorbance of the sample.

The viability of HFF-1 cells was further determined by the calcein acetoxymethyl ester/propidium iodide (calcein-AM/PI) co-stained assay in which the live cells were stained by calcein-AM to development of green color, and the dead cells were stained by PI to red. Briefly, HFF-1 cells were seeded at  $3 \times 10^4$  cells/well into 24-well plates and incubated overnight. After the required treatments and 24 h incubation, the cells were labeled with calcein-AM/PI for 30 min and then were observed with a Laser Scanning Confocal Microscope (Nikon, Japan) at an excitation wavelength of 490 nm.

## Determination of ROS production

Intracellular ROS production was measured using the fluorescent probe, DCFH-DA. HFF-1 cells were seeded at a density of  $1 \times 10^4$  cells/well in 96-well plates with 200  $\mu$ L medium, and incubated overnight. After treatment with E-EA (or Trolox) for 2 h, HFF-1 cells were incubated in 100  $\mu$ mol/L DCFH-DA with 200  $\mu$ L FBS-free medium for 30 min and irradiated with 40 mJ/cm<sup>2</sup> UVB. Intracellular ROS production was measured at 480 nm (excitation) and 525 nm (emission) using a multimode microplate reader. Similarly, HFF-1 cells ( $5 \times 10^5$  cells/well) were seeded in a glass dish and incubated overnight. Cells were treated with E-EA (or Trolox), labeled with DCFH-DA and irradiated with 40 mJ/cm<sup>2</sup> UVB. After irradiation, a laser scanning confocal microscope (Nikon, Japan) was used to view and photograph the HFF-1 cells at an excitation wavelength 488 nm.

## Determination of MMP-1 and type-I procollagen production

MMP-1 and type-I procollagen secreted by HFF-1 cells in culture media were estimated by the enzyme-linked immunosorbent assay (ELISA). Cells with or without E-EA (or Trolox) treatment were irradiated with 60 mJ/cm<sup>2</sup> UVB. The culture media was collected 12 h later. MMP-1 and type-I procollagen were measured using an ELISA kit as recommended by the manufacturer.

## Western blot analysis

The relative amounts of MAPKs in the cell were assessed by Western immunoblotting [20]. HFF-1 cells ( $5 \times 10^5$  cells/well) were seeded in 6-well plates and pretreated with different concentrations of E-EA for 24 h. The cells were exposed to 60 mJ/cm<sup>2</sup> UVB irradiation. At 30 min after irradiation, total cell lysates were extracted and centrifuged. Sixty  $\mu$ L cell lysate in the supernatant were mixed with 15  $\mu$ L loading buffer and boiled for 10 min. The mixture was separated by 12% sodium dodecyl sulfate (SDS) polyacrylamide-gel electrophoresis (PAGE). The separated protein samples were transferred to PVDF membranes. After blocking with 5% BSA, the membranes were first incubated with primary antibodies, and then washed in tris-buffered saline (TBS) and 0.1% Tween 20 (TBST), and finally incubated with secondary antibodies. After washing in TBST, the target

proteins on membranes were detected using enhanced chemiluminescence reagents and imaging system. The protein bands were analyzed using ImageJ software.

### HPLC analysis

HPLC analysis was performed with an Agilent 1260 HPLC system equipped with a Unitary C<sub>18</sub> column (4.6 mm×250 mm, 5.0 μm 100 A, ACCHROM, China). The mobile phase was composed of 0.1% trifluoroacetic acid (TFA) aqueous solution and acetonitrile with gradient elution (0-5 min, 20%-30% acetonitrile; 5-20 min, 30%-45%; 20-25 min, 45%-100%). The solvent flow rate was 1.0 mL/min, the injection volume was 10 μL and the detection wavelength was 360 nm.

### Statistical analysis

Data were expressed as means±SD and evaluated using Student's T-test and SPSS 23 software packages (IBM Corporation, USA). Significance was defined as  $p < 0.05$ ,  $p < 0.01$  and  $p < 0.001$ .

## RESULTS

### Antioxidant activity and total flavonoid content

DPPH and ABTS<sup>+</sup> radical scavenging assays and the total reducing power assay were used to evaluate the *in vitro* antioxidant activity of *Rubus chingii* Hu. extracts (Table 1). DPPH radical scavenging ability, in increasing order, was E-EA>E-NB>E-WR>E. ABTS<sup>+</sup> radical

scavenging ability and the total reducing power were in the order of E-EA>E-NB>E>E-WR. The IC<sub>50</sub> value of E-EA for ABTS<sup>+</sup> radical scavenging ability was 3.18 μg/mL, which was as low as the positive control Trolox. The TFC of the fractions of *Rubus chingii* Hu. was also measured, as shown in Table 1. In these fractions, E-EA contained the highest content of flavonoids, followed by E-NB, E and E-WR.

### UV absorption

E-EA provided strong UV absorption (Fig. 1). Moreover, the UV absorption of E-EA was stronger than that of Trolox at a wavelength range of 200-400 nm.

### E-EA attenuated UVB-induced cytotoxicity

The effect of E-EA on UVB-induced toxicity in HFF-1 cells was assessed by comparing to Trolox in both preventive and therapeutic experiments using the MTT assay. Cytotoxicity against HFF-1 cells was measured to determine the non-toxic dose of E-EA in comparison to Trolox. As can be seen in Fig. 2A, cell viability was higher than 85% when the cells were incubated with E-EA at doses ranging from 0 to 50 μg/mL. The preventive and therapeutic effects of E-EA in HFF-1 cells under UVB irradiation were determined. In the preventive approach, HFF-1 cells were pretreated with E-EA (0, 10, 20, 40 μg/mL) before irradiation with UVB. As shown in Fig. 2B, UVB irradiation reduced the viability of HFF-1 cells to 78.81%. However, the

**Table 1.** TFC, DPPH· and ABTS<sup>+</sup> scavenging activities and the total reducing power of the fractions.

samples	TFC (mg rutin/g)	DPPH·IC <sub>50</sub> (μg/mL)	ABTS <sup>+</sup> IC <sub>50</sub> (μg/mL)	FRAP (g Trolox /g)
E	178.16±0.78 <sup>c</sup>	40.49±0.66 <sup>c</sup>	5.08±0.17 <sup>d</sup>	0.570±0.001 <sup>d</sup>
E-PE	\	> 100	> 100	\
E-EA	275.23±1.20 <sup>a</sup>	9.47±0.03 <sup>b</sup>	3.18±0.08 <sup>a</sup>	0.960±0.002 <sup>b</sup>
E-NB	245.66±1.36 <sup>b</sup>	12.72±0.19 <sup>c</sup>	3.89±0.05 <sup>b</sup>	0.741±0.007 <sup>c</sup>
E-WR	146.76±0.78 <sup>d</sup>	37.12±0.16 <sup>d</sup>	8.72±0.06 <sup>c</sup>	0.335±0.005 <sup>c</sup>
Trolox	\	5.43±0.08 <sup>a</sup>	3.16±0.04 <sup>a</sup>	1.035±0.003 <sup>a</sup>

TFC was expressed as rutin equivalents in mg/g of extract. DPPH· and ABTS<sup>+</sup> radical scavenging activities were expressed as IC<sub>50</sub> (samples at the concentration decrease the absorbance by 50%). FRAP was expressed as Trolox equivalents in g/g of extract. Each value is expressed as the mean±SD (n=3). Means with different letters in a column are significantly different at  $p < 0.001$ . “\” means not determined.

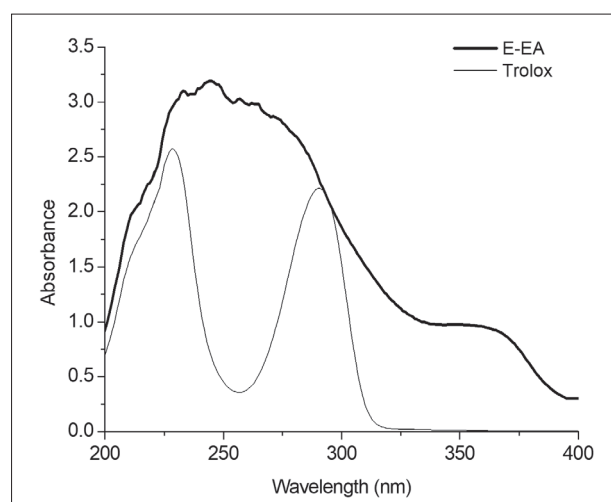


**Fig. 1.** UV absorption spectrum of E-EA and Trolox at 200 μg/mL.

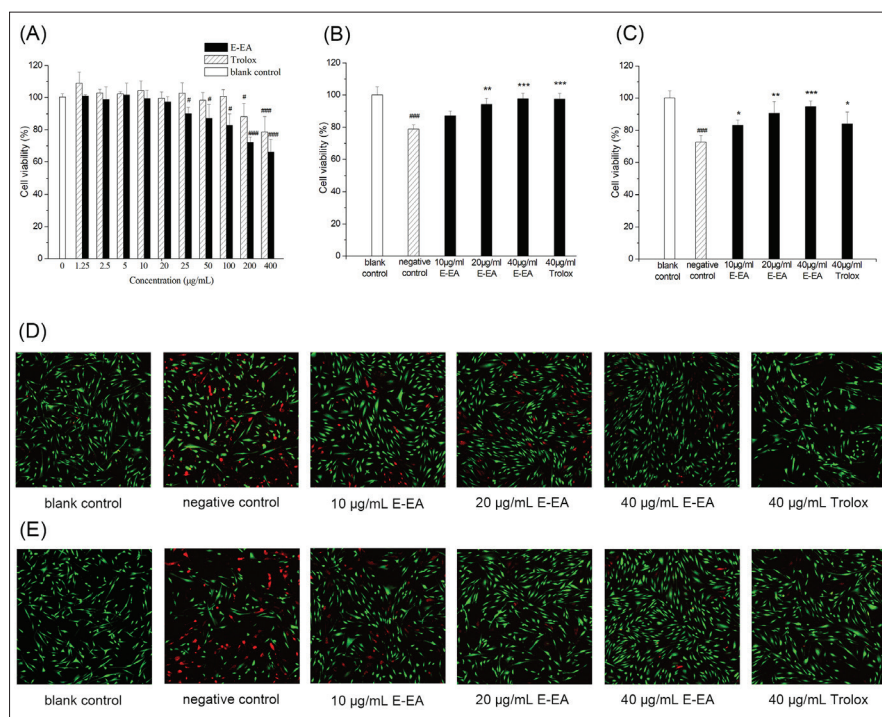


**Fig. 2.** Anti-photoaging effects of E-EA on UVB-induced cytotoxicity in HFF-1 cells. A – Effect of E-EA on proliferation of HFF-1 cells after treatment for 24 h. B – Preventive effect of E-EA on UVB-induced cytotoxicity in HFF-1 cells. HFF-1 cells were pretreated with different concentrations of E-EA and Trolox for 24 h and irradiated with 60 mJ/cm<sup>2</sup> UVB. C – Therapeutic effect of E-EA on UVB-induced cytotoxicity in HFF-1 cells. HFF-1 cells were irradiated with 60 mJ/cm<sup>2</sup> UVB and treated with different concentrations of E-EA and Trolox for 24 h. Cell viability was measured by MTT assay. D – Confocal images of calcein AM (green)/PI (red) co-stained HFF-1 cells in a preventive assay. E – Confocal images of calcein AM (green)/PI (red) co-stained HFF-1 cells in a therapeutic assay. Data are expressed as the mean±SD (n=3) (###*p*<0.001, #*p*<0.05 versus blank control; \*\*\**p*<0.001, \*\**p*<0.01, and \**p*<0.05 versus negative control).

viability of HFF-1 cells after pretreatment with 10, 20, 40 µg/mL E-EA increased to 87.19%, 94.09% and 97.62%, respectively. In the therapeutic approach, HFF-1 cells were initially irradiated with UVB and then treated with E-EA (0, 10, 20, 40 µg/mL). From Fig. 2C it can be seen that the viability of UVB-induced HFF-1 cells increased from 72.56% to 83.00%, 90.43% and 94.55%, respectively after treatment with 10, 20, 40 µg/mL E-EA. The change in cell viability with or without UVB irradiation and E-EA treatment is also illustrated in Fig. 2D-E by the calcein-AM/PI co-staining assay. The results are in accordance with those of the MTT assay. Many dead cells (red) were observed in the UVB irradiation group. The treatment with E-EA caused a decrease in the amount of dead cells in both the preventive and therapeutic approaches. Furthermore, the percentage of viable cells (green) increased with the increase in E-EA concentration.

### E-EA reduced UVB-induced intercellular ROS generation

Monitoring the intracellular ROS level in HFF-1 cells was used to investigate the effects of E-EA on UVB-induced photoaging. As shown in Fig. 3A, UVB irradiation stimulated an increase in the intracellular ROS

levels in HFF-1 cells from 47.62% to 100%. When HFF-1 cells were pretreated with E-EA, the increase in ROS levels induced by UVB was alleviated. The intracellular ROS labeled with DCFH-DA were also photographed using a laser scanning confocal microscope. Fig. 3B showed that the highest fluorescence intensity was observed in cells induced by UVB (negative control). The fluorescence intensity of HFF-1 cells pretreated with E-EA was reduced.

### E-EA inhibited UVB-induced MMP-1 secretion and increased type-I procollagen expression

In order to further determine the anti-photoaging activity of E-EA, the effects of increasing concentrations (0, 10, 20, 40 µg/mL) of E-EA on UVB-induced MMP-1 expressions and type-I procollagen degradation were measured. As can be seen in Fig. 4, compared with the blank control, the expression of MMP-1 was increased by 36.50%, and type-I procollagen expression was decreased by 15.63% in HFF-1 cells after UVB irradiation. However, when cells were pretreated with 20 and 40 µg/mL E-EA, MMP-1 expression was inhibited by 24.27% (\*\**p*<0.001) and 23.90% (\*\**p*<0.001), respectively, and type-I procollagen recovered by 7.81% (\**p*<0.05) and 12.93% (\*\**p*<0.01), respectively, as compared to

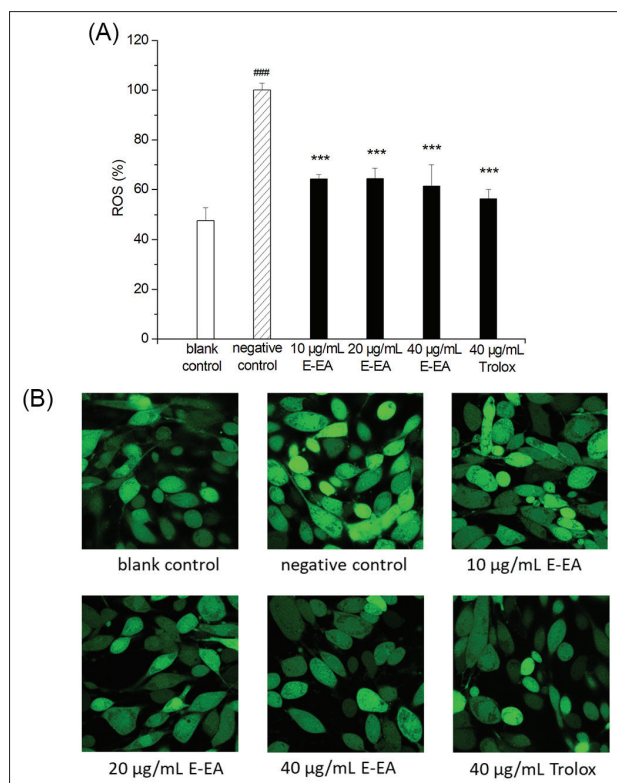


**Fig. 3.** Effect of E-EA on intracellular ROS generation in UVB-induced HFF-1 cells. A – ROS level was measured using a multi-mode microplate reader. B – ROS level was photographed using a laser scanning confocal microscope. HFF-1 cells were pretreated with different concentrations of E-EA and Trolox for 2 h, labeled with DCFH-DA for 30 min and irradiated with 40 mJ/cm<sup>2</sup> UVB. Data are expressed as the mean±SD (n=3) (###*p*<0.001 versus blank control; \*\*\**p*<0.001 versus negative control)

the negative control. Interestingly, the recovery effects of E-EA for UVB-induced MMP-1 and procollagen I production were better than the effect of Trolox at a concentration of 40 µg/mL.

### E-EA suppressed UVB-induced MAPK pathway activation

To determine the biological effects of E-EA on MAPK signaling pathways, which likely regulated the UVB-induced expression of MMP-1 and type-I procollagen, we examined the relative changes in phosphorylated ERK, JNK and p38 protein levels examined by Western immunoblotting. As shown in Fig. 5, the phosphorylation levels of MAPKs (ERK, JNK and p38) in UVB-induced HFF-1 cells (negative controls) were increased compared to the controls. However, pretreatment of

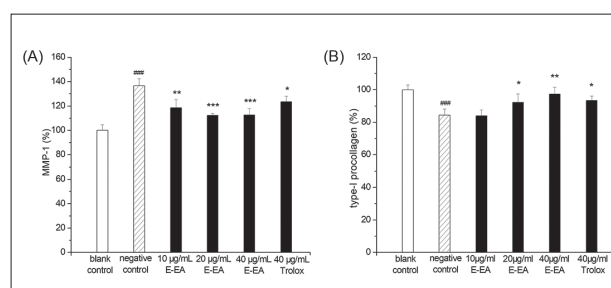


**Fig. 4.** Effects of E-EA on (A) MMP-1 suppression and (B) type-I procollagen expression in UVB-induced HFF-1 cells. HFF-1 cells were pretreated with different concentrations of E-EA and Trolox for 24 h and irradiated with 60 mJ/cm<sup>2</sup> UVB. At 12 h after UVB treatment, the culture medium was collected and MMP-1 and type-I procollagen were measured. Data are expressed as the mean±SD (n=3) (###*p*<0.001 versus blank control; \*\*\**p*<0.001, \*\**p*<0.01 and \**p*<0.05 versus negative control)

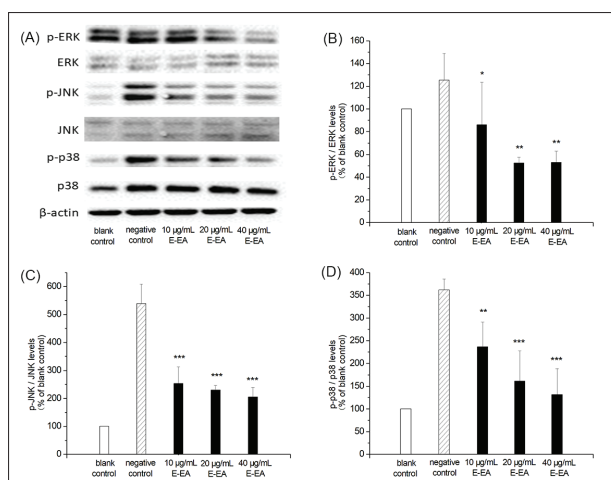


**Fig. 5.** Effects of E-EA on MAPK signaling pathway suppression in UVB-induced HFF-1 cells. The cultured HFF-1 cells were pretreated with E-EA for 24 h and then irradiated with 60 mJ/cm<sup>2</sup> UVB. Western immunoblotting (30 min after UVB treatment): A – MAPK pathway; B – p-ERK/ERK; C – p-JNK/JNK; D – p-p38/p38 expression. β-actin was used as an internal control. Data are expressed as the mean±SD (n = 3) (\*\*\**p*<0.001, \*\**p*<0.01, and \**p*<0.05 versus negative control)

HFF-1 cells with 10, 20 and 40 µg/mL of E-EA resulted in strong decreases in the ratios of p-ERK/ ERK, p-JNK/ JNK and p-p38/ p38 band intensities.

### The HPLC analysis of E-EA

The representative flavonoids rutin, hyperin, quercetin and kaempferol were used as standard substances to characterize the chemical composition of E-EA. Fig.

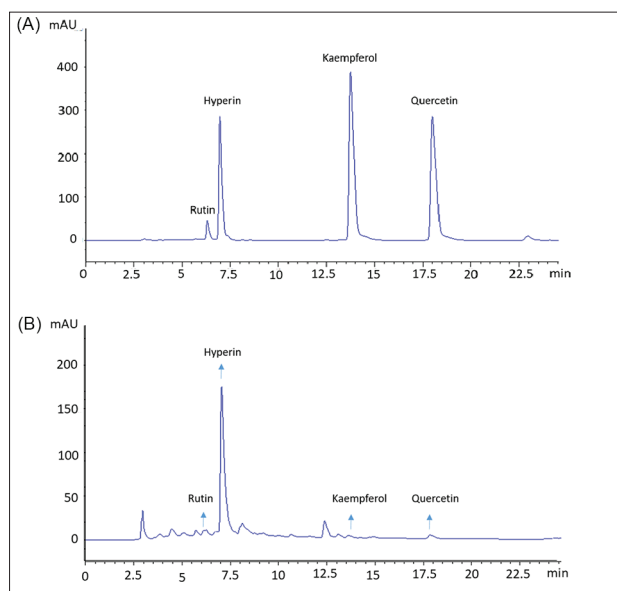


**Fig. 6.** HPLC analysis of (A) four flavonoid standards and (B) E-EA. The flavonoid compounds were identified by comparing their retention times.

6 shows that all four flavonoids could be detected by HPLC in E-EA, of which the contents of rutin and hyperin in E-EA were 2.65 mg/g and 69.33 mg/g, respectively. The contents of the other two compounds in E-EA were less than 0.75 mg/g.

## DISCUSSION

Increases in intracellular free radical levels are closely associated with cell senescence, thus free radical scavenging ability is a potential target for aging prevention [1]. In this work, all fractions, except E-PE, exhibited antioxidant activity in a dose-dependent manner within concentrations of 1.25-100  $\mu\text{g}/\text{mL}$ . The E-EA fraction had the best antioxidant capacity in the five fractions of *Rubus chingii* Hu., which was in agreement with previous literature [14]. The anti-aging properties of plants are attributed to contained antioxidant substances, such as polyphenols, flavonoids and anthocyanins [5]. Flavonoids are ubiquitous plant secondary products that exhibit a variety of biological activities and are beneficial to human health [21,22]. In our work, the highest flavonoid content was found in E-EA, suggesting that flavonoids were excellent antioxidants. Several other plant extracts, including *Juniperus communis* L., *Hypericum organifolium* Willd. are widely documented as effective anti-aging agents

because of their high flavonoid and high polyphenol contents [23,24]. The flavonoids contained in plants possess potent antioxidant properties and strong UV absorption, and are widely used in skin protection [1,25]. This suggests that E-EA with its high flavonoid content and strong UV absorption might also provide photoaging resistance for skin care.

It is well known that UVB significantly reduces the viability of human fibroblasts [26]. However, plant extracts can effectively reduce the cytotoxicity of UVB. For example, polyphenol extracts from *Hawthorn Crataegus* L. and hesperidin extract from *Zanthoxylum rhetsa* have been reported to possess a preventive or therapeutic effect on UVB-induced cell death in human dermal fibroblasts [4, 27]. In the present study, UVB irradiation remarkably reduced HFF-1 cell viability in both preventive and therapeutic assays. In the preventive approach, pretreatment with E-EA attenuated the UVB-induced cytotoxicity in HFF-1 cells. In particular, when treated with E-EA at a concentration of 40  $\mu\text{g}/\text{mL}$ , cell viability was recovered to the level of the control group. Furthermore, in the therapeutic approach, UVB-induced HFF-1 cell damage was effectively repaired by E-EA. When the concentration of E-EA was 20 and 40  $\mu\text{g}/\text{mL}$ , cell viability was higher than obtained with 40  $\mu\text{g}/\text{mL}$  Trolox. These results indicated that the E-EA fraction exhibited excellent preventive and therapeutic effects against UVB-induced cell damage in HFF-1 cells.

UVB-induced ROS overproduction is directly related to the occurrence of skin photoaging [2]. The intracellular ROS level of HFF-1 cells irradiated with UVB was significantly increased. The extent of intracellular ROS increase was significantly reduced when HFF-1 cells were pretreated with E-EA at test concentrations (10-40  $\mu\text{g}/\text{mL}$ ) ( $p < 0.001$ ). These results showed that E-EA prevented HFF-1 cells from UVB-induced ROS overproduction. Similarly, plant extracts such as clove, sea buckthorn seed and hawthorn have previously been reported to inhibit the production of ROS after UVB induction [27-29]. Aging is associated with cell damage from ROS, and reducing ROS production might be one of the effective strategies to prevent cell aging. Thus, E-EA has the potential to protect the skin against UVB-induced photoaging by reducing ROS overproduction.

ROS overproduction activates the MAPK signaling pathways, which stimulates the transcription of MMP-1 genes in fibroblasts and negatively regulates the transcription of genes encoding type-I procollagen [30]. The results presented herein showed that UVB could significantly upregulate MMP-1 expression and downregulate type-I procollagen in HFF-1 cells via activation of the MAPKs, including ERK, JNK and p38. Nevertheless, treating UVB-induced HFF-1 cells with E-EA significantly decreased the phosphorylation of ERK, JNK and p38, which resulted in the attenuation of MMP-1 production and recovery of type I procollagen expression [31]. These results suggest that E-EA has the ability to protect skin from UVB-induced photoaging by downregulating MMP-1 expression and upregulating type-I procollagen production via inhibition of MAPKs.

Flavonoids act as ROS scavengers because of their abundance in hydroxyl groups [30]. Hyperin was determined to be a major compound in *Rubus chingii* Hu. fruit by HPLC analysis, which is consistent with a previous report [13]. Hyperin has been identified as an antioxidant with ROS scavenging ability that can enhance skin density and elasticity by mediating MMP-1 and type-I procollagen expression [32]. We speculate that the antioxidant and anti-photoaging effects of E-EA are due to the hyperin.

To conclude, our study demonstrated that E-EA, which contains hyperin as a major active compound, was capable of protecting HFF-1 cells from UVB-induced photoaging by scavenging free radicals and reducing ROS levels, decreasing MMP-1 expression and recovering type-I procollagen production via suppression of the activation of MAPKs. The presented results suggest that E-EA can effectively protect the skin from UVB damage and that it has potential applications in cosmetics.

**Acknowledgment:** This work was supported in part by the Fundamental Research Funds for Central Universities, No. 222201817022.

**Author contributions:** LM and YH designed the research study. SJ, SZ and YH performed the research. SJ, SZ and JZ performed the statistical analysis. SJ and YH performed the first drafting of the manuscript. All authors read and approved the manuscript.

**Conflict of interest disclosure:** The authors have no financial interests or potential conflicts of interests to declare.

## REFERENCES

1. Gragnani A, Cornick SM, Chominski V, Ribeiro de Noronha SM, Alves Corrêa de Noronha SA, Ferreira LM. Review of major theories of skin aging. *Adv Aging Res.* 2014;03(04):265-84.
2. Cavinato M, Jansen-Durr P. Molecular mechanisms of UVB-induced senescence of dermal fibroblasts and its relevance for photoaging of the human skin. *Exp Gerontol.* 2017;94:78-82.
3. Lee CH, Wu SB, Hong CH, Yu HS, Wei YH. Molecular mechanisms of UV-induced apoptosis and its effects on skin residential cells: the implication in UV-based phototherapy. *Int J Mol Sci.* 2013;14(3):6414-35.
4. Santhanam RK, Fakurazi S, Ahmad S, Abas F, Ismail IS, Rukayadi Y, Akhtar MT, Shaari K. Inhibition of UVB-induced pro-inflammatory cytokines and MMP expression by *Zanthoxylum rhetsa* bark extract and its active constituent hesperidin. *Phytother Res.* 2018;32(8):1608-16.
5. Chiocchio I, Mandrone M, Sanna C, Maxia A, Tacchini M, Poli F. Screening of a hundred plant extracts as tyrosinase and elastase inhibitors, two enzymatic targets of cosmetic interest. *Ind Crop Prod.* 2018;122:498-505.
6. Lu J, Guo JH, Tu XL, Zhang C, Zhao M, Zhang QW, Gao FH. Tiron inhibits UVB-induced AP-1 binding sites transcriptional activation on MMP-1 and MMP-3 promoters by MAPK signaling pathway in human dermal fibroblasts. *PLoS One.* 2016;11(8):e0159998.
7. Gilchrist BA. Photoaging. *J Invest Dermatol.* 2013;133(E1):E2-6.
8. Zeng HJ, Liu Z, Wang YP, Yang D, Yang R, Qu LB. Studies on the anti-aging activity of a glycoprotein isolated from Fupenzi (*Rubus chingii* Hu.) and its regulation on klotho gene expression in mice kidney. *Int J Biol Macromol.* 2018;119:470-6.
9. Rowland J, Akbarov A, Eales J, Xu X, Dormer JP, Guo H, Deniff M, Jiang X, Ranjzad P, Nazgiewicz A, Prestes PR, Antczak A, Szulinska M, Wise IA, Zukowska-Szczechowska E, Bogdanski P, Woolf AS, Samani NJ, Charchar FJ, Tomaszewski M. Uncovering genetic mechanisms of kidney aging through transcriptomics, genomics, and epigenomics. *Kidney Int.* 2019;95(3):624-35.
10. Li G, Chen Y, Hu H, Liu L, Hu X, Wang J, Shi W, Yin D. Association between age-related decline of kidney function and plasma malondialdehyde. *Rejuven. Res.* 2012;15(3):257-64.
11. Schmidlin CJ, Dodson MB, Madhavan L, Zhang DD. Redox regulation by NRF2 in aging and disease. *Free Radic Biol Med.* 2019;134:702-4.
12. Yau M-H, Che C-T, Liang S-M, Kong Y-C, Fong W-P. An aqueous extract of *Rubus chingii* fruits protects primary rat hepatocytes against tert-butyl hydroperoxide induced oxidative stress. *Life Sci.* 2002;72(3):329-38.
13. Zeng H, Yang R, Lei L, Wang Y. Total flavonoid content, the antioxidant capacity, fingerprinting and quantitative analysis of fupenzi (*Rubus chingii* Hu.). *Chin Med.* 2015;06(04):204-13.
14. Zhang TT, Liu YJ, Yang L, Jiang JG, Zhao JW, Zhu W. Extraction of antioxidant and antiproliferative ingredients from fruits of *Rubus chingii* Hu by active tracking guidance. *Medchemcomm.* 2017;8(8):1673-80.
15. Zhang TT, Wang M, Yang L, Jiang J-G, Zhao J-W, Zhu W. Flavonoid glycosides from *Rubus chingii* Hu fruits display anti-

- inflammatory activity through suppressing MAPKs activation in macrophages. *J Funct Foods*. 2015;18:235-43.
16. Brand-Williams W, Cuvelier ME, Berset C. Use of a free radical method to evaluate antioxidant activity. *LWT - Food Sci Technol*. 1995;28(1):25-30.
  17. Re R, Pellegrini N, Proteggente A, Pannala A, Yang M, Rice-Evans C. Antioxidant activity applying an improved ABTS radical cation decolorization assay. *Free Radic Biol Med*. 1999;26(9-10):1231-7.
  18. Stanic-Vucinic D, Prodic I, Apostolovic D, Nikolic M, Velickovic TC. Structure and antioxidant activity of beta-lactoglobulin-glycoconjugates obtained by high-intensity-ultrasound-induced Maillard reaction in aqueous model systems under neutral conditions. *Food Chem*. 2013;138(1):590-9.
  19. Meyers KJ, Watkins CB, Pritts MP, Liu RH. Antioxidant and antiproliferative activities of strawberries. *J Agric Food Chem*. 2003;51(23):6887-92.
  20. Xuan SH, Park YM, Park SH, Jeong HJ, Park SN. Suppression of Ultraviolet B-mediated matrix metalloproteinase generation by *Sorbus commixta* Twig extract in human dermal fibroblasts. *Photochem Photobiol*. 2018;94(2):370-7.
  21. Vauzour D, Rodriguez-Mateos A, Corona G, Oruna-Concha MJ, Spencer JP. Polyphenols and human health: prevention of disease and mechanisms of action. *Nutrients*. 2010;2(11):1106-31.
  22. Prochazkova D, Bousova I, Wilhelmova N. Antioxidant and prooxidant properties of flavonoids. *Fitoterapia*. 2011;82(4):513-23.
  23. Pandey S, Tiwari S, Kumar A, Niranjana A, Chand J, Lehri A, Chauhan PS. Antioxidant and anti-aging potential of Juniper berry (*Juniperus communis* L.) essential oil in *Caenorhabditis elegans* model system. *Ind Crop Prod*. 2018;120:113-22.
  24. Boran R. Investigations of anti-aging potential of *Hypericum origanifolium* Willd. for skincare formulations. *Ind Crop Prod*. 2018;118:290-5.
  25. Saewan N, Jimtaisong A. Photoprotection of natural flavonoids. *J App Pharm Sci*. 2013;3(09):129-41.
  26. Zakaria NNA, Okello EJ, Howes MJ, Birch-Machin MA, Bowman A. In vitro protective effects of an aqueous extract of *Clitoria ternatea* L. flower against hydrogen peroxide-induced cytotoxicity and UV-induced mtDNA damage in human keratinocytes. *Phytother Res*. 2018;32(6):1064-72.
  27. Liu S, You L, Zhao Y, Chang X. Hawthorn polyphenol extract inhibits UVB-induced skin photoaging by regulating MMP expression and Type I Procollagen production in mice. *J Agric Food Chem*. 2018;66(32):8537-46.
  28. Kim H, Cho H, Seo Y-K, Kim S, Yoon MY, Kang H, Park CS, Park JK. Inhibitory effects of sea buckthorn (*Hippophae rhamnoides* L.) seed on UVB-induced Photoaging in human dermal fibroblasts. *Biotechnol Bioprocess Eng*. 2012;17(3):465-74.
  29. Hwang E, Lin P, Ngo HTT, Yi TH. Clove attenuates UVB-induced photodamage and repairs skin barrier function in hairless mice. *Food Funct*. 2018;9(9):4936-47.
  30. Li L, Hwang E, Ngo HTT, Lin P, Gao W, Liu Y, Yi TH. Anti-photoaging effect of *Prunus yeonesis* Blossom extract via inhibition of MAPK/AP-1 and regulation of the TGF- $\beta$ 1/Smad and Nrf2/ARE signaling pathways. *Photochem Photobiol*. 2018;94(4):725-32.
  31. Duque L, Bravo K, Osorio E. A holistic anti-aging approach applied in selected cultivated medicinal plants: A view of photoprotection of the skin by different mechanisms. *Ind Crop Prod*. 2017;97:431-9.
  32. Huang CY, Lin YT, Kuo HC, Chiou WF, Lee MH. Compounds isolated from *Eriobotrya deflexa* leaves protect against ultraviolet radiation B-induced photoaging in human fibroblasts. *J Photochem Photobiol B: Biol*. 2017;175:244-53.